Investigation of the Chemical Purity of Silicon Surfaces Reacted with Liquid Methanol

David J. Michalak,[†,§] Sandrine Rivillon Amy,[†,⊥] A. Estève,[‡] and Yves J. Chabal*[,†,∥]

Department of Chemistry and Chemical Biology, Rutgers University, Piscataway, New Jersey 08502, Department of Materials Science and Engineering, University of Texas at Dallas, Richardson, Texas 75080, and Laboratoire d'Analyse et d'Architecture des Systèmes-CNRS, University of Toulouse, 31077 Toulouse, France

Received: April 8, 2008

The reaction of hydrogen-terminated Si(111) and oxide-terminated silicon surfaces with neat anhydrous liquid methanol (CH_3OH) has been studied with Fourier transform infrared spectroscopy (FTIR) as a function of solution temperature and immersion time. At 65 °C, reaction of atomically smooth H−Si(111) surfaces with CH_3OH (l) results in partially methoxylated silicon surfaces that are free of any detectable subsurface oxidation (Si−O−Si bonds); this is in contrast to observable oxidation found after similar reactions on H−Si(100) surfaces. At long reaction times ($t > 3$ h), the Si(111) surface saturates with Si-OCH_3 sites at a coverage of approximately 30% of a monolayer, with the residual ~70% comprised of unreacted Si−H sites. The lack of any detectable silicon oxide makes it possible to conclude the following: (i) Reaction mechanisms involving insertion of oxygen atoms from the CH_3OH molecule into the subsurface Si−Si back bonds cannot be dominant for (111)-oriented silicon under these conditions. (ii) The vibrational modes of the oxide-free surface are very sharp and can be clearly distinguished from blue-shifted modes observed for methoxyl groups chemisorbed on oxidized surfaces. For surfaces that display subsurface oxidation, no evidence for oxygen atoms directly below atop Si−H sites has been observed. Instead, FTIR analysis demonstrates that subsurface oxidation selectively exists underneath atop Si-OCH_3 sites. Finally, H-terminated oxide surfaces, prepared by reacting trichlorosilanes on OH-terminated SiO_2 surfaces, react with methanol to form a methoxy-terminated oxide surface.

I. Introduction

Careful chemical control over surfaces is important for the next generation of semiconductor devices. As device sizes get smaller, the surface-area-to-volume ratio increases, and custom control over the surface chemistry is required in order to optimize the desired performance. For example, untreated subsurface oxidation often compromises the performance of electronic devices[1–3] and optical sensors[4,5] and is particularly important for small devices such as nanowires.[6] Chemical modification[7,8] is used to form surfaces of high electrical quality that resist oxide growth.[9–17] Surface chemistry can also be employed to adjust the electrical performance by modifying interfacial electron transfer kinetics[17–20] and/or to adjust the dominant electron−hole recombination mechanisms.[21,22] Chemical modification of silicon or silica surfaces with functional end groups is also employed for antistiction coatings in devices for microelectromechanical systems (MEMS)[23–25] or to enable specific binding interactions to relevant molecules or proteins for various sensing applications.[4,16,26–31] Despite the wide applicability of surface chemistry, the chemical stability of functionalized surfaces is, however, of concern because they are often stable only over a limited working range of temperature,[32,33] air composition, physiological conditions,[5] or pH values.[34] Thus, understanding the chemical behavior of silicon surfaces with regard to the chemical and electrical stability is important for future technological developments.

At the atomic level, chemical modification of the surface occurs through the formation of Si−C, Si−O, or, occasionally, Si−N bonds.[35–37] It is the stability of these "first bonds" that determines the stability of the interface and electrical performance. Although the Si−C bond is not too strong from a thermodynamic standpoint, the surfaces that result from these terminations appear incredibly inert,[9,13–15,38] most likely for kinetic reasons. Si−O bonds are more thermodynamically stable, and chemical functionalization based on Si−O linkages are ubiquitous in surface adsorbed monolayer (SAM) applications[4,16,34,39–44] because of the ease in forming such surfaces. Such linkers are attached through reaction of the surface with alcohols,[45–51] aldehydes,[45,52,53] and chloro- or alkoxy-silanes.[4,16,42,43] There is considerable concern about the oxidation of the underlying silicon surface; in some cases, the oxidation dominates the SAM binding process, and surfaces must be preoxidized and bonded to large adsorbates in order to achieve stability.[4,16]

We have chosen a system that allows the fundamentals of silicon surface chemistry to be investigated at a very high level of resolution. First, atomically smooth hydrogen-terminated Si(111) surfaces have been used because of the simplicity and homogeneity of the surface. Proper etching of Si(111) surfaces leads to atomically smooth terraces (covering more than 99% of the surface), which contain a homogeneous array of identical Si−H bonds oriented normal to the surface.[54] This surface thus provides essentially only one reactant, which simplifies the number of possible reaction products. Second, the choice of methanol is critical. It is the smallest molecule, hence with the

* To whom correspondence should be addressed. E-mail: chabal@utdallas.edu.
† Rutgers University.
∥ University of Texas at Dallas.
‡ University of Toulouse.
§ Current address: Department of Chemistry, University of California, Berkeley, Berkeley, CA 94720.
⊥ Current address: Material Research Center, Air Products and Chemicals Inc., Allentown, PA 18195.

10.1021/jp8030539 CCC: $40.75
Published on Web 07/16/2008

fewest number of vibrational modes, that contains both a hydrophobic (CH_3) terminus and a hydrophilic (OH) terminus. In addition to acting as a model for the variety of OH-containing chemicals used in the formation of many SAMs, alcohols such as methanol are also important as rinsing agents or as reaction solvents. In some cases, the use of alcohols as solvents has been shown to compete with the preferred reaction pathway.[55] Additionally, alcohols are often added to various etching solutions in order to break the surface tension and allow for desired structures (of certain porosity) to be made;[4,16,56,57] in these situations, the surface interaction with the alcohol is significant.[58] Methanol can thus act as a suitable model to understand fundamental surface chemistry for a number of relevant applications. Third, advances in data acquisition technology have allowed Fourier transform infrared spectroscopy to probe bonding interactions of submonolayer surface species with high resolution. Thus, it is the combination of the homogeneity of the H−Si(111) surface, the broadband sensitivity of transmission mode FTIR, and the spectral simplicity of methanol that allows new insights in surface chemistry to be obtained.

We have previously shown using FTIR analysis that neat anhydrous liquid methanol reacts with H-terminated silicon surfaces,[59] but important questions about the reaction mechanism as well as the position of the observed oxidation still remain. This paper systematically investigates the methoxylation reaction on both H-terminated and oxidized Si surfaces. Specifically, we determine the optimum conditions for forming a uniform submonolayer coverage of methoxyl groups without any detectable silicon oxide ($<\sim$3% of a monolayer).[60] Such surfaces, achieved by $\geq$3 h immersion in methanol at 65 °C, display a maximum of $\sim$30% of a monolayer of Si-OCH_3 sites interspersed between the remaining $\sim$70% of a monolayer of Si−H sites. We also study the physical location of the subsurface oxidation that forms under certain conditions. Finally, we demonstrate that trichlorosilane-derivatized oxide-terminated surfaces also exhibit relatively high reactivity with methanol.

II. Experimental Section

A. Materials and Methods. Anhydrous methanol (CH_3OH) (99.8%), trichlorosilane (TCS, 99%), and anhydrous toluene were purchased from Aldrich. These chemicals were used as received and were placed inside a N_2(g)-purged glovebox prior to use. Aqueous ammonium fluoride (40% by weight) and aqueous hydrofluoric acid (49% by weight) were obtained from J.T. Baker. Aqueous hydrogen peroxide (30% by weight) and concentrated (18 M) sulfuric acid were obtained from EM science. CAUTION: *concentrated sulfuric acid is highly toxic and corrosive and can cause serious burns. Fluoride-containing solutions such as 11 M (40% by weight) NH_4F, buffered HF, and 27 M (48% by weight) HF pose a serious contact hazard. Hydrofluoric acid is highly toxic and corrosive and may cause serious burns which may not be immediately painful or visible. Fluoride ions readily penetrate the skin and can cause destruction of deep tissue and bone.* All H_2O is deionized with a resistivity of 18.2 MΩ cm.

N-type (phosphorus-doped, resistivity $\sim$24−34 Ω-cm) float-zone Si(111) wafers, polished on both sides, were cut into 2 cm × 5 cm pieces for transmission mode infrared analysis. P-type (boron doped, resistivity 10 Ω-cm) float-zone Si(100) wafers, also polished on both sides, were obtained with an initially grown 25−60 Å thick terminating oxide. These oxide-terminated samples were cleaned using the RCA procedure that involved a 10 min exposure to an 80 °C SC1 solution (4:1:1 H_2O:30% H_2O_2(aq):concentrated NH_4OH(aq)), followed by a rinsing step using 1 L of H_2O, a 10 min exposure to an 80 °C SC2 solution (4:1:1 H_2O:30% H_2O_2(aq):concentrated HCl(aq)), and a final rinsing step using 1 L of H_2O. Si(100) samples were hydrogen-terminated by a 30 s dip in 10−20% HF(aq) followed by a 10 s H_2O rinse. Si(111) samples were hydrogen-terminated by a 30 s dip in 10−20% HF(aq) followed by a 2.5 min dip in 40% NH_4F(aq), and a final rinse in H_2O for 10 s. This latter procedure produces an atomically smooth (111)-oriented surface for tens to hundreds of nanometers.[54,61,62] Oxides were chemically grown on an atomically flat hydrogen-terminated Si(111) surface using either the SC1/SC2 procedure outlined above or a 10 min exposure to 100 °C solution of 4:1 concentrated (18 M) H_2SO_4:30% H_2O_2(aq) (hereafter referred to as piranha solution). Oxide surfaces grown from the piranha clean typically produced FTIR spectra that exhibited less hydrocarbon contamination. Silicon samples of (111)-orientation were often reused since an atomically flat surface could be prepared between subsequent experiments. Si(100) surfaces were not reused since continued HF(aq)-etching and oxidation steps could increase the surface roughness.

Data were recorded in the dry N_2(g)-purged bench of a Fourier transform infrared (FTIR) spectrometer (Nicolet 6700, Nexus 670, Magna 860). Spectra were obtained with a nominal 4 cm^{-1} resolution between 400 and 4000 cm^{-1} in transmission mode, at an angle of incidence of 74° (Brewster angle for silicon) with respect to the Si surface normal. A room temperature pyroelectric detector (DTGS) was used for data collection. Five consecutive loops, each consisting of 1000 single beam spectral scans, were obtained for each sample. References were either oxide-terminated or freshly etched hydrogen-terminated surfaces, as appropriate. The absorbance spectra were processed by subtracting water vapor and CO_2(g) peaks and then by flattening the baseline to remove drifts. Omnic software was used to integrate the peak areas, and, when appropriate, peaks were fitted using Origin software.

Reactions were performed in 2.5 cm diameter × 15 cm glass tubes. These tubes were initially cleaned with aqua regia, followed by a 10 min clean with piranha solution to remove traces of metallic and carbon-containing contamination from the surfaces of the glass. The tubes were then rinsed with copious H_2O, fully dried using a heat gun, and brought into a nitrogen glovebox. For reactions performed at elevated temperatures, the tubes were placed into an aluminum heating block with a 2.6 cm diameter × 5 cm deep hole that fit the tube such that a silicon sample could be heated evenly along its entire length. The temperature of the solution was measured by a thermocouple probe that was placed between the tube and the aluminum block, and a feedback controller was used to keep the temperature constant. Separate reaction tubes were used for methanol and TCS/toluene solutions. A glass tube containing a given reaction solution was preheated to the temperature of interest for about 30 min before discarding that solution as a rinse waste. In addition to removing any impurities, this high temperature rinse would chemically modify the surface of the glass tube to be either methoxy-terminated (for methanol reactions) or hydrogen-terminated (for TCS/toluene reactions). Another allotment of solution was added subsequently and preheated to the desired temperature before the silicon sample was added. After immersion of the sample into the liquid, the tube was wrapped quickly with Al foil which provided both darkness (to minimize the effect of photogenerated charge carriers on the reaction rates) and thermal insulation. After the desired reaction time, the sample and solution were poured into

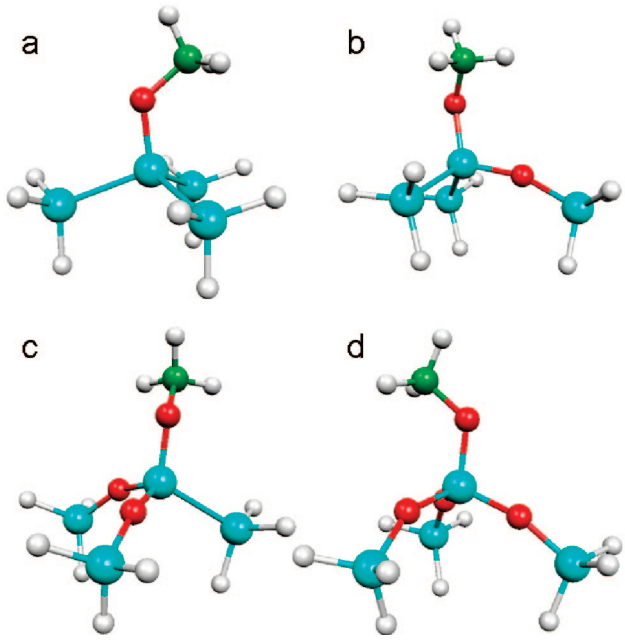

Figure 1. Models used in the calculations of infrared active modes for atop Si−OCH_3 groups containing either (a) zero, (b) one, (c) two, or (d) three oxygen atoms in the Si−Si back bonds: Si (blue), O (red), C (green), and H (white).

a glass funnel, where the Si sample quickly dried. For reactions near room temperature, it was often necessary to angle and wave the sample to encourage evaporation of the liquid down to a corner of the sample that was not probed by FTIR. Once dry, samples were capped in centrifuge tubes under N_2(g), removed from the glovebox, and carried to the spectrometer. When not in use, reaction tubes were capped with rubber stoppers, to prevent cross contamination, and stored in the glovebox.

B. First-Principles Calculations. All calculations were performed at the density functional level of theory using the Gaussian 03 package.[63] All geometries and subsequent frequency determinations were calculated within the combined Becke's three parameters exchange hybrid functional B3LYP associated with the generalized gradient approximation (GGA) of Lee, Yang, and Parr.[64,65] The electronic wave functions were described by the 6-31+G** basis set. The cluster used to model the surface was composed of two silicon layers (4 atoms) with their valency satisfied by hydrogen atoms. The Si−H bonds oriented toward the third subsurface layer were restricted to motions along the bulk Si−Si crystal lattice directions in order to more closely mimic a real surface section and to allow for a precise definition of its normal orientation. The high frequency CH stretching region was scaled with reference to experimental Si−H modes, having a typical scaling factor of 0.95 compared to calculated values. For the scaling studies involving the Si−H terminal cluster, the three second-layer silicon atoms were terminated by D atoms, to prevent coupling interactions. The geometries and vibration frequencies were subsequently determined for a cluster model in which one, two, or three oxygen atoms were inserted into each of one, two or, three Si−Si backbonds to the second layer of silicon atoms (Figure 1). The positions of the three subsurface silicon atoms were not fixed in the models containing subsurface oxygen atoms. For this reason, the Si−O−Si bonds of these models are not as strained as they would be for a real Si(111) surface with local patches of oxidation.

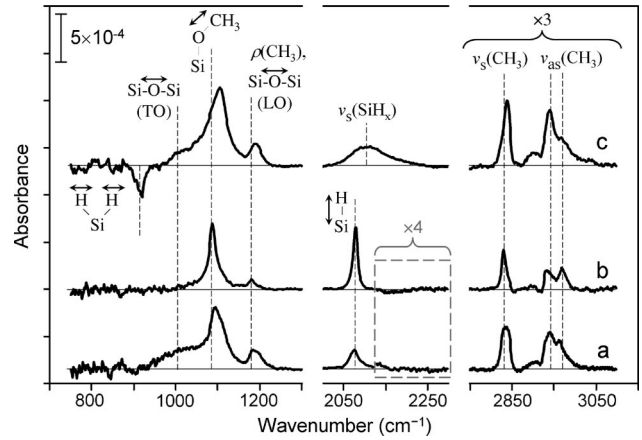

Figure 2. FTIR spectra of atomically smooth H−Si(111) samples after exposure to CH_3OH (l) in the dark for (a) 6 days at room temperature or (b) 12 h at 65 °C or for (c) a H−Si(100) sample exposed to CH_3OH (l) in the dark for 3 h at 65 °C. The spectra for the H−Si(100) surface and the room-temperature-reacted H−Si(111) surface present observable subsurface oxidation (Si−O−Si LO and TO modes), whereas no detectable oxide is observed upon reaction of H−Si(111) with 65 °C CH_3OH (l). The single beam spectra are referenced relative to the native oxide-terminated surface within the spectral region of 2000−2300 cm^{-1} and are referenced relative to the atomically smooth H−Si(111) surface in the spectral regions of 750−1300 and 2800−3100 cm^{-1}.

III. Results

In an attempt to optimize the methoxylation reaction with H-terminated Si surfaces, i.e., to minimize the formation of SiO_2, we first explore the solution temperature and immersion time in methanol. We then study the methoxylation of oxidized surfaces, including hydroxy- and hydrogen-terminated SiO_2 surfaces.

A. Reactions of H−Si(111) Surfaces with Methanol. Similar to recent results,[59] Figure 2a displays the FTIR spectrum of an atomically smooth H−Si(111) sample after exposure to CH_3OH (l) in the dark for 6 days at room temperature. The exchange of some atop Si−H groups with atop Si−OCH_3 groups is demonstrated by the appearance of a CH_3 symmetric (∼2840 cm^{-1}) and two CH_3 asymmetric (∼2940 and ∼2980 cm^{-1}) stretching modes, a decrease in the intensity of, and a red-shift in, the Si−H stretching mode (∼2080 cm^{-1}), the appearance of the CH_3 umbrella distortion (1190 cm^{-1}), and the appearance of a complex mode involving an O−C stretching motion coupled with a C−H bending motion (∼1090 cm^{-1}).[47,49,50,59,66] The broadening (the full width at half-max increases up to 20 cm^{-1}) and red-shifting (by about 6 cm^{-1}) of the remaining Si−H stretching modes indicates that dipole−dipole coupling between neighboring Si−H species is being disrupted.[67–70] This observation is consistent with random exchange of Si−H sites to Si−OCH_3 sites over the entire surface rather than the formation of separated domains of isolated Si−H and Si−OCH_3 groups. There is observable oxidation of the silicon surface as evidenced by positive absorption modes at ∼1050 $cm^{-1}$and ∼1220 cm^{-1}, which correspond to the asymmetric Si−O−Si transverse optical (TO) and Si−O−Si longitudinal optical (LO) stretching modes, respectively.[71] The frequency of the LO mode indicates that the regions of oxide (SiO_2) are very small in physical size,[72,73] possibly including as few as 10 oxygen atoms.[74] This is consistent with scanning tunneling microscopy observations that oxidation of H−Si(111) surfaces occurs in randomly distributed 10−20 Å diameter domains.[75] Similar results have been found for the oxidation of ethyl-terminated Si(111) surfaces using scanning Auger microscopy.[15] Interestingly, the Si−O−Si

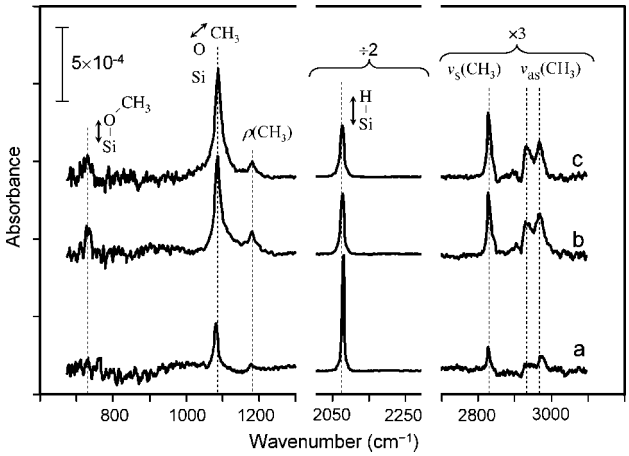

Figure 3. FTIR spectra of hydrogen-terminated *n*-Si(111) surfaces immersed in neat anhydrous CH_3OH (l) in the dark at 65 °C for (a) 10 min, (b) 3 h, and (c) 12 h. The reaction appears to be nearly complete after 3 h (Table 1). The single beam spectra are referenced relative to the native oxide-terminated surface within the spectral region of 2000−2300 cm^{-1} and are referenced relative to the atomically smooth H−Si(111) surface in the spectral regions of 750−1300 and 2800−3100 cm^{-1}.

oxidation species observed in Figure 2a do not reside underneath surface-bound Si−H sites, because there is no observable absorption in the 2100−2300 cm^{-1} range, which corresponds to Si−H species with oxygen inserted in the Si−Si back bonds (hereafter referred to as O_xSi−H species);[76] this spectral region is multiplied by a factor of 4 for the spectra of Figure 2, panels a and b, for clarity. Based on the spectral noise rms of $(5 \pm 1) \times 10^{-6}$ and an estimated signal-to-noise ratio of 4 necessary for detection, the O_xSi−H species must be less than 4% of a monolayer. While the amount of oxidation observed on these samples is variable, it is consistently larger than 4% of a monolayer (typically 30−100% of a monolayer for room temperature reactions), implying that O_xSi−H species should be observed out of the noise if the oxidation resides below Si−H sites. The absence of O_xSi−H modes in this study is in contrast with experiments on H−Si(111) samples exposed to gas-phase O_2 or H_2O at elevated temperatures.[76] These results imply that different oxidation pathways exist between higher-temperature gas phase and lower-temperature solution phase systems.

When the H−Si(111) surface is exposed to 65 °C CH_3OH (l) in the dark for 12 h, no detectable SiO_2 modes are observed[77] despite a similar $\nu_s(CH_3)$ intensity (similar $Si-OCH_3$ coverage) relative to the 6 day room-temperature reaction (c.f., Figure 2, panels a and b, and the data in Table 1). In addition, the complex O−C mode, the CH_3 umbrella mode, the residual Si−H stretching mode, and the C−H stretching modes are all significantly spectrally sharper. The spectrum obtained after reaction of a hydrogen-terminated Si(100) surface with 65 °C CH_3OH (l) for 3 h in the dark is presented in Figure 2c for comparison. Although this spectrum presents visibly larger C−H stretching and larger complex O−C modes, suggesting a higher coverage of $Si-OCH_3$ sites,[78] the modes are considerably broader with clearly detectable subsurface oxidation even under the same reaction conditions (e.g., oxygen- and water-contamination levels, temperature, and darkness) as the Si(111) surface of Figure 2b. The negative mode at 911 cm^{-1} (Figure 2c) is assigned to a loss in the SiH_2 scissor mode (relative to the freshly etched hydrogen-terminated Si(100) surface used as a reference for this spectral region) due to reaction of the dihydride surface species with methanol. Correspondingly, the 2000−2300 cm^{-1} Si−H stretching region (relative to the oxide surface) is very broad after reaction as it contains modes corresponding to coupled and uncoupled SiH−, SiH_2−, and SiH_3−stretching modes[79,80] in a variety of chemical environments.

TABLE 1: Stretching Mode Areas[a] for H−Si(111) as a Function of Reaction Time in CH_3OH (l)

surface treatment	frac. Si−H coverage[b]	complex O−C (mAU cm^{-1})	$\nu_s(CH_3)$ (mAU cm^{-1})
freshly etched	1	0	0
65 °C Rxn:			
10 min CH_3OH	0.90 ± 0.04	6 ± 1	1.6 ± 0.4
3 h CH_3OH	0.77 ± 0.05	23 ± 1	2.5 ± 0.2
10−12 h CH_3OH	0.72 ± 0.03	22 ± 3	2.9 ± 0.6
Room Temp Rxn:			
10 min CH_3OH	0.94 ± 0.13		0.7 ± 0.2
3 h CH_3OH	0.85 ± 0.10	12 ± 2	1.2 ± 0.4
24 h CH_3OH	0.73 ± 0.06	25 ± 3	1.6 ± 0.4
6 day CH_3OH[c]	0.56 ± 0.10	21 ± 7	3.2 ± 2.2

[a] The areas were evaluated for a 74° angle of incidence relative to the surface normal, with the aperture 100% open, and exciting roughly 4 cm^2 of the surface of the sample. The front and rear face of the surface are treated identically and both are absorbing light. [b] The fractional Si−H coverage values were calculated as the ratio of the area of the H−Si stretching mode after a given surface treatment (referenced relative to the oxide spectrum of that sample) to the area under the initial freshly etched H−Si stretching mode of that same sample (referenced relative to the oxide spectrum). [c] The fractional Si−H coverage below 0.7 is most likely attributed to the large amount of oxidation also observed on these samples and does not necessarily imply a higher $Si-OCH_3$ coverage. The $\nu_s(CH_3)$ mode areas are assumed to produce a more reliable comparison of the $Si-OCH_3$ coverage.

Figure 3 displays the FTIR spectra of hydrogen-terminated *n*-Si(111) samples immersed in neat anhydrous CH_3OH (l) in the dark at 65 °C after reaction times of 10 min, 3 h, or 12 h. This study of immersion time shows that the complex O−C, Si−H, and C−H stretching modes remain sharp with no detectable SiO_2 modes over a wide range of reaction times; there are also no large shifts in the resonant frequencies. As opposed to the room temperature study previously reported,[59] these spectra are obtained with a lower-noise detector that made it possible to observe the weak Si−O stretching mode at 734 cm^{-1} (predicted by previous DFT calculations to be at ~725 cm^{-1}).[59] Table 1 displays the area of the Si−H, C−H, and complex O−C modes for each reaction time; the reaction with 65 °C neat methanol appears to be nearly complete after 3 h.

B. Reactions of Oxide Surfaces with Methanol. Although the subsurface oxide found on the room-temperature-reacted surfaces (Figure 2a) does not appear to reside below atop Si−H sites, it could reside directly below atop $Si-OCH_3$ sites. FTIR analysis was performed on oxidized silicon surfaces in order to observe any changes in the stretching frequencies for such $Si-OCH_3$ sites (hereafter referred to as $O_xSi-OCH_3$ sites). Figure 4 presents the FTIR spectra of a thin wet-chemically generated 5−10 Å thick oxide-terminated *n*-Si(111) surface immersed in neat anhydrous CH_3OH (l) for 3 h at 65 °C. This oxide layer was generated by treating an atomically flat hydrogen-terminated Si(111) surface with a 10 min immersion in piranha solution. Figure 4a displays the low frequency absorbance spectrum of the CH_3OH-treated oxide surface relative to the initial oxide surface. Spectra b and c represent the piranha-grown oxide surface (gray) and the CH_3OH-treated oxide surface (black) each referenced relative to the initial atomically flat H−Si(111) surface; both are divided by a factor of 2 and superimposed for clarity. Spectra b and c are included to demonstrate that the broad mode around ~1050 cm^{-1} and

TABLE 2: Observed and Calculated Modes for the Unoxidized $Si_3Si-OCH_3$ and Oxidized $O_xSi-OCH_3$ Species

spectral assignment	υ_{obs}	υ_{theo}	intensity[a]	angle[b]	orientation[c]	υ_{obs}	υ_{theo}(1/2/3 O in the backbonds)	intensity[a]
	unoxidized $Si-OCH_3$ (12 h reaction at 65 °C)					oxidized $O_3Si-OCH_3$ (3 h reaction at 65 °C)		
$\upsilon_a(CH_3)$	2972	2941	weak (32)	33°	⊥	2992	2948/2948/2949	w/m/m
$\upsilon_a(CH_3)$	2935	2890	weak (38)	89°	⊥	2956	2912/2912/2915	w/w/w
$\upsilon_s(CH_3)$	2833	2850	med (69)	76°	⊥	2854	2861/2864/2868	m/w/w
$\delta_s(CH_3)$	1180	1182	weak (28)	56°	⊥	1205	1185/1191/1198	w/m/w
$\upsilon(C-O) + \rho(CH_3)$	1088	1077	strong (263)	12°	⊥	1115	1077/1096/1107	vs
Si−O	730	728	weak (64)		⊥	845	765/787/819	s

[a] Intensities calculated from the cluster model are presented in parentheses and are reported in units of km/mol. Calculated intensity values cannot be compared qualitatively between the high and low frequency regions. The Si−O mode at 728 cm^{-1} produces some displacements in the underlying Si atoms and prevent an accurate evaluation of the intensity. [b] This refers to the angle the net dipole moment for a given mode makes relative to the surface normal. The angles were obtained from DFT calculations by summing the products of the atomic displacements and atomic charges. [c] Orientation refers to the experimentally observed orientation of the modes through angle-resolved FTIR measurements. The symbol, ⊥, means that the modes are oriented nearly perpendicular to the surface; since light-incidence angles of only 74 and 10° off normal were used, the experimental results cannot give more precision in the orientation.

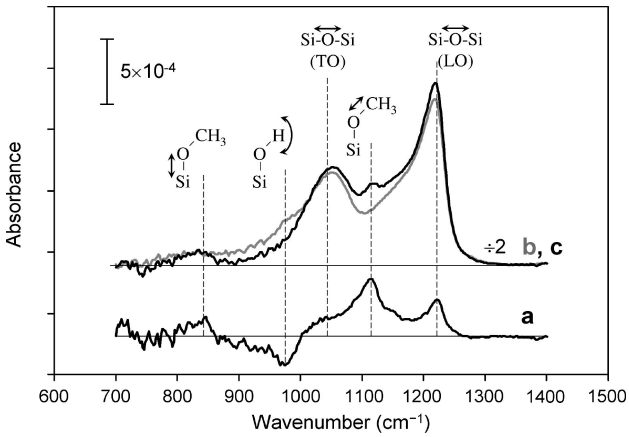

Figure 4. FTIR spectra of a 5−10 Å thick oxide-terminated *n*-Si(111) surface immersed in neat anhydrous CH_3OH (l) for 3 h at 65 °C. Spectrum a represents the CH_3OH-treated oxide surface referenced to the initial oxide. Spectra b and c (divided by a factor of 2 for clarity) are the oxide surface (gray) and the CH_3OH-treated surface (black), respectively, both referenced relative to an oxide-free H−Si(111) surface.

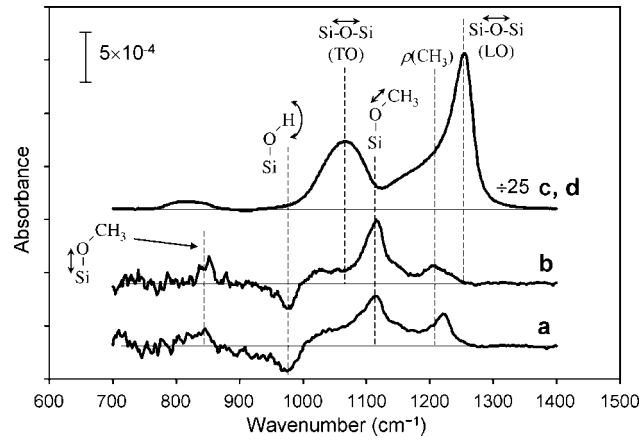

Figure 5. FTIR spectra of a 25−60 Å thick oxide-terminated Si(100) surface immersed in neat anhydrous CH_3OH (l) for 3 h at 65 °C. Spectrum a is reproduced from Figure 4a (thin chemical oxide). Spectra b–d represent the reaction on the 25−60 Å thick oxide surface. Spectrum b represents the CH_3OH-treated oxide surface referenced to the initial oxide. Spectra c and d are the oxide (gray) and the CH_3OH-exposed oxide (black) surfaces (referenced relative to an oxide-free H−Si(100) surface). Spectrum b is not complicated by changes in the asymmetric Si−O−Si TO or LO modes, which allows the $Si-OCH_3$ umbrella mode, $\rho(CH_3)$, to be observed at 1205 cm^{-1}.

the sharp peak at 1220 cm^{-1} of Figure 4a can be assigned to increases in the asymmetric Si−O−Si TO and LO stretching modes of the surface oxide layer, respectively. This increase in the TO and LO modes is either due to an increase in the oxide thickness, via continued oxidation, or to an increase in the structural order of the oxide, or both. In addition to the TO and LO modes, positive absorbance features associated with the complex O−C mode at 1118 cm^{-1} and a Si−O stretch around 845 cm^{-1} are observed, as well as a negative feature ascribable to a loss in the SiO−H bending mode at 977 cm^{-1} (Figure 4a). Importantly, the complex O−C and Si−O stretching modes are blue-shifted by 30 cm^{-1} and over 100 cm^{-1} respectively on the oxide surface (Figure 4a) relative to what is observed on the oxide-free $Si-OCH_3$ surface (Figure 2b). One $\upsilon_s(CH_3)$ and two $\upsilon_a(CH_3)$ modes (not shown) appear at 2854, 2956, and 2992 cm^{-1}, respectively, and are roughly 20 cm^{-1} blue-shifted relative to those observed on the nominally oxide-free Si(111) surface (Figure 2b).

In order to eliminate spectral features due to changes in the thin surface oxide layer during the reaction with CH_3OH, the same reaction was carried out on Si(100) samples with a thermally generated 25−60 Å thick oxide layer provided by the commercial vendor. Figure 5 displays the low frequency FTIR results obtained for the reaction of this oxide-terminated Si(100) surface with neat anhydrous CH_3OH (l) for 3 h at 65 °C. For comparison, the spectrum of Figure 4a (thin wet-chemical oxide) is reproduced as Figure 5a. Spectrum Figure 5b is the absorbance spectrum generated by referencing the CH_3OH-treated 25−60 Å thick Si(100) oxide surface relative to the initial oxide. Spectra c and d in Figure 5 are the initial 25−60 Å thick oxide surface (gray), and the CH_3OH-exposed oxide surface (black), respectively, each referenced relative to the oxide-free H−Si(100) surface that was created at the end of the experiment. The significantly thicker oxide layer produces asymmetric Si−O−Si TO and LO modes at 1050 and 1260 cm^{-1}, respectively, that are not only much stronger in intensity (requiring division of the spectra by 25 for clarity) but the LO mode is significantly blue-shifted in frequency compared to the thinner oxide.[71] The weaker mode at ∼820 cm^{-1} on spectra 5c and 5d represents the unresolved TO and LO pair of the symmetric Si−O−Si stretching modes.[73] The absence of modes at 1050 and 1260 cm^{-1} on spectrum 5b demonstrates that no changes in the oxide layer occurred during the reaction with CH_3OH, and thus the umbrella mode, $\rho(CH_3)$, of the methoxyl group is now apparent at ∼1205 cm^{-1}. Comparison of the spectra obtained on oxides of different thicknesses (Figure 5, spectra a and b) shows that, despite the spectral changes associated with the TO and LO modes of the thinner oxide, the peaks ascribable to the complex O−C mode, SiO−H bending mode, and the Si−O stretch do not change in frequency.

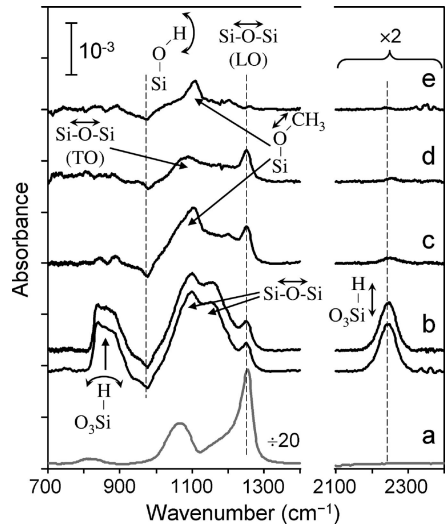

Figure 6. FTIR spectra of a hydrogen-terminated oxide surface after various reactions. Figure 6a presents the initial 25−60 Å thick oxide-covered Si(100) surface relative to an oxide-free H−Si(100) surface. Spectrum b presents the oxide surface after exposure to the TCS solution before and after sonication. Subsequent reaction of the surface with 65 °C CH_3OH for 10 min (spectrum c) significantly reduces the TCS-formed O_3Si-H and Si−O−Si modes and forms $O_3Si-OCH_3$ species. Selective exchange of $Si-OCH_3$ groups with Si−OH groups occurs after exposure of the surface to a 5 min SC2 solution (spectrum d). Spectrum e represents the CH_3OH-reacted surface referenced relative to the final SC2-cleaned surface (see text for more details). All spectra within the region of 2100−2400 cm^{-1} are multiplied by a factor of 2.

C. Reaction of Hydrogen-Terminated Oxide Surfaces with Methanol. Despite the occurrence of the SiO_2 on the room-temperature-reacted $Si-OCH_3$ surface (Figure 2a), no evidence for the presence of O_xSi-H species are observed. Such O_xSi-H species could be formed transiently, however, provided a fast reaction of these sites with CH_3OH ensues. In order to investigate this possibility, the reaction of hydrogen-terminated oxide surfaces with CH_3OH (l) was studied. Such surfaces were generated by immersing an oxide-terminated sample in a 35 °C solution of trichlorosilane, Cl_3Si-H (TCS, 99%), in anhydrous toluene (∼15 mM, or 40−60 μL TCS in 30 mL toluene) for 6 h. A simplified reaction can be written as follows, where the subscript s represents the surface bound species.[87]

$$Cl_3SiH + 3H_2O \rightarrow (HO)_3SiH + 3HCl \quad (1)$$

$$n\mathrm{Si_sOH} + (HO)_3SiH \rightarrow (\mathrm{Si_sO})_n(HO)_{(3-n)}SiH + nH_2O \quad (2)$$

In the first step, the TCS molecule undergoes hydrolysis with H_2O molecules that are either in solution or physisorbed to the surface of the oxide layer. In the second step, the hydrolyzed TCS molecule undergoes some number, ($1 \le n \le 3$), of condensation reactions with a corresponding number of Si−OH surface groups; the remaining hydrolyzed sites of the TCS molecule either remain as Si−OH groups or they may undergo condensation with neighboring, or incoming, hydrolyzed TCS molecules.

Figure 6 displays the low frequency FTIR spectra for hydrogen-terminated oxide surfaces with methanol. In Figure 6a, the spectrum of the 25−60 Å thick oxide-terminated Si(100) wafer, which was the starting surface for subsequent chemistry, is displayed relative to the oxide-free hydrogen-terminated Si(100) surface formed upon completion of the experiment; this spectrum (divided by 20) is included to show the frequencies of the Si−O−Si LO (1260 cm^{-1}) and TO (1050 cm^{-1}) modes for comparison. The lower spectrum of Figure 6b displays the absorbance spectrum after immersion of the initial oxide in a 35 °C solution of TCS in toluene for 6 h in the dark; this spectrum is referenced relative to the initial oxide surface. The positive absorbance modes around 850 and 2245 cm^{-1} correspond to the Si−H bending and stretching modes, respectively, for the O_3Si-H species; for all spectra, absorbance values between 2100 and 2400 cm^{-1} are multiplied by 2 for clarity. The 2245 cm^{-1} O_3Si-H stretching mode displays an area of ∼0.027 AU cm^{-1}. Assuming the O_3Si-H and (111)Si−H species have similar oscillator strengths, the (111)Si−H area of ∼0.014 AU cm^{-1} implies that the TCS film is roughly two monolayers thick. The negative feature at 977 cm^{-1} is due to the loss of surface-atop Si−OH species from reaction with hydrolyzed TCS molecules.[82] The positive mode at 1260 cm^{-1} corresponds to the generation of Si−O−Si species that are coupled to the Si−O−Si LO mode of the surface oxide (c.f. Figure 6a). The positive modes between 1050 and 1200 cm^{-1} correspond to new Si−O−Si modes that are isolated (not coupled) to the bulk LO mode. The upper spectrum of Figure 6b was obtained after the surface was sonicated for 10 min in toluene to remove any physisorbed Si−O−Si oligomers deposited from solution-phase condensation of TCS molecules.[81] Since there is no statistical difference in areas of these two spectra, we conclude that negligible amounts of condensation products were physisorbed to this particular sample; thus, all observed Si−O−Si modes are assumed to be directly bound to the surface in some form.

Figure 6c displays the absorbance spectrum of the H-terminated oxide surface after a 10 min reaction in 65 °C CH_3OH (l) in the dark (referenced relative to the initial oxide surface). The stretching and bending modes for O_3Si-H species almost completely disappear with only 10 ± 4% of the initial O_3Si-H groups remaining. This is in stark contrast to the ≈90% Si−H remaining on the H−Si(111) surface under the same reaction conditions (Figure 3a, Table 1). In addition to the loss of the O_3Si-H modes, a significant proportion of the uncoupled Si−O−Si modes (between 1050 and 1200 cm^{-1}) have disappeared while the Si−O−Si species that coupled to the Si−O−Si LO mode (∼1260 cm^{-1}) remain relatively unchanged. The significant loss of the uncoupled Si−O−Si modes (1050−1200 cm^{-1}) is in stark contrast to the negligible loss of oxide-layer-coupled Si−O−Si modes (1250 cm^{-1}). This indicates a surprising difference in the reactivity of these two types of Si−O−Si species. As evidence for the formation of $O_xSi-OCH_3$ groups, small positive modes at 1115 and 1205 cm^{-1} are assigned to the complex O−C and CH_3 umbrella modes.

Figure 6d displays the spectrum obtained after dipping the CH_3OH-exposed surface into an SC2 solution for 5 min (the initial oxide surface is used as a reference). The acidic SC2 solution is assumed to only hydrolyze the atop $Si-OCH_3$ groups into Si−OH groups while not affecting the Si−O−Si groups. Accordingly, Figure 6d demonstrates that the complex O−C (1115 cm^{-1}) and umbrella CH_3 (1205 cm^{-1}) modes, that were present in Figure 6c, disappear. The frequencies of the remaining Si−O−Si modes (1050 and 1260 cm^{-1}) compare well to the Si−O−Si LO and TO modes of Figure 6a. Figure 6e presents the spectrum of the CH_3OH-reacted surface relative to the surface generated after the final SC2 clean. The positive absorbance features thus represent the chemical species removed during the SC2 cleaning. The negative mode at 977 cm^{-1} means that Si−OH sites are formed upon the loss of $Si-OCH_3$ sites.

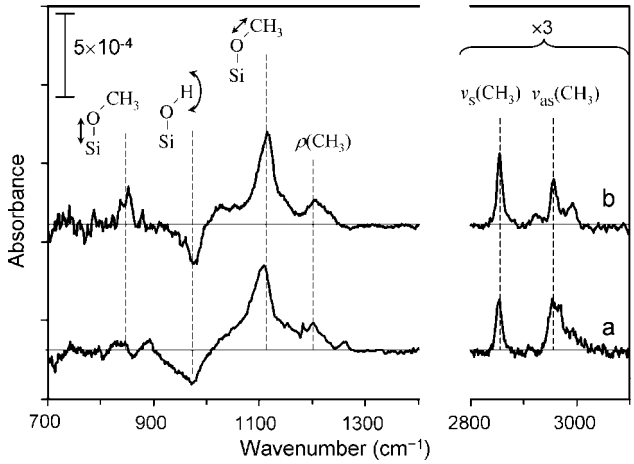

Figure 7. FTIR spectra of (a) a hydrogen-terminated oxide (O_3Si-H) sample (from Figure 6e) and (b) a hydroxy-terminated oxide (O_3Si-OH) sample (from Figure 5b) after reaction in 65 °C CH_3OH. The C−H stretching region is also included. The similar spectral features and intensities indicate that the resulting surfaces are very similar despite the difference in the initial surface chemistry.

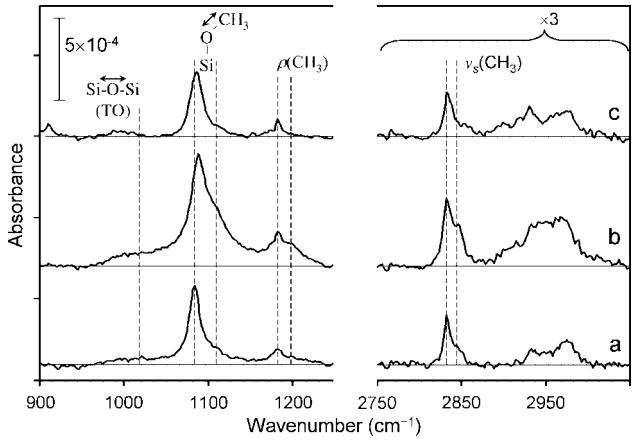

Figure 8. FTIR spectra of a deliberately oxidized methoxy-terminated sample. An atomically smooth hydrogen-terminated *n*-Si(111) sample was sequentially exposed to (a) neat anhydrous methanol for 3 h at 65 °C, (b) dark air for 14 h, followed by 10 h in 65 °C methanol, and finally (c) 37 s in 48% HF(aq). Correlated with the appearance of oxidation (Si−O−Si TO) are blue-shifted components of the complex O−C, $\rho(CH_3)$, and $\nu_s(CH_3)$ modes (spectrum b). The Si−O−Si TO and blue-shifted components are both significantly reduced upon exposure to 48% HF(aq) (spectrum c), whereas the non-blue-shifted components are relatively unaffected. All spectra are referenced relative to the initial atomically smooth H−Si(111).

The spectrum is very similar to that obtained after reacting the bare 25−60 Ang Si(100) oxide surface with CH_3OH for 3 h (Figure 5b).

The CH_3OH-reacted hydrogen-terminated oxide surface (of Figure 6e) and the CH_3OH-reacted hydroxy-terminated oxide surface (of Figure 5b) are reproduced in Figure 7 along with the C−H stretching region for comparison. The spectral features and intensities of both spectra are very similar (including the $\nu_s(CH_3)$ mode at 2854 cm^{-1}) despite the difference in the initial surface chemistry. The spectra in Figures 4–7 and the data summarized in Table 2 demonstrate that the modes associated with surface-bound $O_xSi-OCH_3$ group are blue-shifted on oxidized silicon surfaces relative to those on oxide-free Si(111) surfaces.

D. Deliberate Oxidation of Methoxylated Surfaces. An oxide-free methoxylated surface was deliberately oxidized in air to observe any shifts in the Si−OCH_3 vibration modes. The

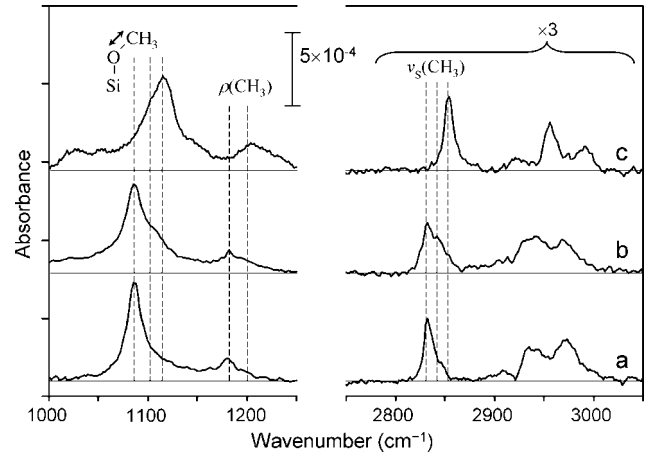

Figure 9. Comparison of spectral features for different CH_3O-terminated surfaces: (a) a flat H−Si(111) exposed to 65 °C CH_3OH (l) for 3 h, (b) a flat H−Si(111) exposed to room temperature CH_3OH (l) for 6 days, and (c) a 25−60 Å thick oxide surface exposed to 65 °C CH_3OH (l) for 3 h. The sharp modes of the virtually oxide free surface of spectrum a are the lowest in frequency. Significant blue-shifted components of the same modes are observed for the oxide-containing room-temperature reacted surface (b). The modes are the most blue-shifted on an oxide surface (c).

spectrum of Figure 8a demonstrates that the initial Si−OCH_3 surface, formed after immersion in 65 °C methanol is free of significant SiO_2.[83] The surface was subsequently oxidized through a 14 h exposure to laboratory air in the dark followed by a 10 h reaction in 65 °C methanol (Figure 8b). Subsurface oxidation is verified by the appearance of a Si−O−Si TO mode (∼1020 cm^{-1}). In addition, observable blue-shifted components of the complex O−C, CH_3 umbrella, and $\nu_s(CH_3)$ modes of Si−OCH_3 groups also appear. These blue-shifted components, as well as the Si−O−Si TO mode, are significantly reduced upon the subsequent dip of the surface in 27 M HF(aq) for 37 s (Figure 8c). These results demonstrate that the Si−O−Si oxidation and blue-shifted Si−OCH_3 modes are strongly correlated. (See the Supporting Information section for more analysis.) These results also demonstrate that non-blue-shifted (subsurface-oxide-free) Si−OCH_3 groups are more chemically inert to 27 M HF(aq) than the blue-shifted Si−OCH_3 groups, which are presumably located above regions of subsurface oxide that are undercut and removed by the aqueous HF. Consistently, the appearance of the mode at 911 cm^{-1}, which is assigned to a dihydride (SiH_2) mode, is evidence for surface roughening due to the removal of oxidation by HF(aq).

The assignment of blue-shifted modes to $O_xSi-OCH_3$ species is highlighted in Figure 9, where the spectra from several different surfaces are plotted together for comparison. Figure 9a is a spectrum of a flat H−Si(111) exposed to 65 °C CH_3OH for 3 h in the dark, and there are no detectable Si−O−Si modes with only negligible components of the blue-shifted complex O−C, umbrella CH_3, and $\nu_s(CH_3)$ stretching modes; this spectrum thus presents one of the least oxidized samples. The positions of the oxide-free modes at 1088, 1180, and 2833 cm^{-1} for the complex O−C, umbrella CH_3, and $\nu_s(CH_3)$ stretching modes, respectively, are indicated by broken lines. Figure 9b represents a flat H−Si(111) surface exposed to room temperature CH_3OH (l) for 6 days in the dark. The blue-shifted modes are indicated by broken lines at 1105, 1190, and 2843 cm^{-1} for the complex O−C, umbrella CH_3, and $\nu_s(CH_3)$ stretching modes, respectively. This sample also displays a visible Si−O−Si TO mode (1050 cm^{-1}), which is illuminated by the straight line drawn near the baseline. Figure 9c (also Figure 5b) presents

the spectrum for the 25−60 Å thick oxide-terminated Si(100) surface exposed to CH_3OH at 65 °C for 3 h in the dark. This spectrum demonstrates that the complex O−C, umbrella CH_3, and $\upsilon_s(CH_3)$ modes, indicated by broken lines at 1115, 1205, and 2854 cm^{-1}, respectively, are the most blue-shifted on a fully oxidized surface.

E. Theoretical Calculations. Results from the DFT calculations are displayed in Table 2. Consistent with the experimental results, DFT calculations demonstrate that atop $Si-OCH_3$ vibrational modes are blue-shifted by an amount related to the number of O atoms in the back bonds. The experimentally observed stretching frequencies are also presented in Table 2 for the nominally oxide-free ($Si_3Si-OCH_3$) surface as well as for the 25−60 Å thick-oxide-terminated ($O_3Si-OCH_3$) surface. Interestingly, the amount of the shift is proportional to the closeness of the particular vibrational mode to the subsurface oxygen atoms. For example, the experimentally observed shift in the Si−O mode from the unoxidized surface to the oxide-terminated surface is 115 cm^{-1}, and a shift of 85 cm^{-1} is predicted by DFT calculations. For the complex O−C mode, an experimentally observed (DFT-calculated) shift of 27 cm^{-1} is observed (22 cm^{-1} predicted). For the C−H stretching modes, an experimentally observed shift of ∼20 cm^{-1} for each mode is similar to the results predicted by DFT calculations. These trends in blue-shifting are not surprising because the presence of the oxygen atoms in the back bonds will likely have a stronger charge polarizing effect on the Si−O bond than on the more physically remote O−C and C−H bonds.

IV. Discussion

A. Methoxy-Terminated Silicon. The spectra presented in this work highlight several important aspects of silicon surface chemistry. First, hydrogen-terminated Si(111) surfaces can be functionalized via a wet-chemical technique up to ∼30% of a monolayer with direct Si−O linkages without the formation of any detectable SiO_2 (Figures 2b and 3). This is important because high-temperature gas phase reactions of O_2 on H−Si(111) surfaces or of H_2O deposition, and subsequent annealing of, reconstructed Si(100) surfaces demonstrate a high preference of subsurface Si−Si back-bonds to oxidize[84] via an oxygen insertion mechanism.[76,85,86] Thus, there is concern that atop Si−O linkages will be unstable toward decomposition via oxygen diffusion into the back bonds and result in electrically defective subsurface oxidation. Although this sort of decomposition has been demonstrated at elevated temperatures,[71,87] this work shows that a suitable wet-chemical technique can produce surface atop Si−O linkages without subsurface oxidation. Consistently, electrically passive methoxy-terminated Si surfaces, produced through a different wet-chemical technique, have notably long photoinjected charge carrier lifetimes under nitrogen[3,88] and good current−voltage behavior when implemented as silicon photoelectrodes.[22,46,89] Thus, the formation of the Si−O linkages can, in principle, provide an easy functionalization route on Si(111)-oriented wafers that is not complicated by issues of catalysis[55] or the necessity of multistep reactions while nevertheless maintaining good surface electrical properties. Interestingly, the same chemical treatment of 65 °C CH_3OH on Si(100) wafers consistently led to significant subsurface oxidation. These results are consistent with the higher oxidation kinetics measured for the Si(100) surface relative to the Si(111) surface.[76,86] These results provide strong motivation for the use of Si(111) surfaces over Si(100) surface for those electronic devices where atomically smooth, more-controllable, and less-reactive surfaces are needed.

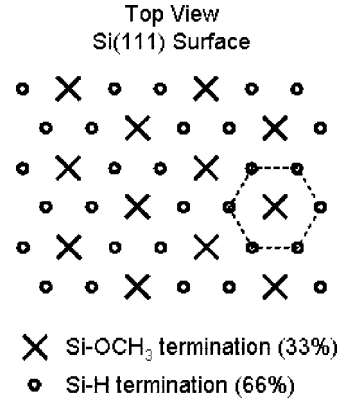

Figure 10. Top-view schematic of the silicon (111) surface with a periodic coverage of 66% Si−H (circles) and 33% $Si-OCH_3$ (crosses). The broken-line hexagon shows that the saturation coverage (Table 1) can be represented as a $Si-OCH_3$ moiety surrounded entirely by nearest-neighbor Si−H groups. Nearest neighbor sites could be sterically inhibited from reaction by the 360° thermal rotation of the methyl group about the Si−O bond.

The saturation coverage of methoxyl species at ∼30% of a monolayer is of particular interest. This coverage of $Si-OCH_3$ sites is close to a 33% coverage, which can be envisioned as a periodic array of $Si-OCH_3$ sites (crosses) surrounded by six nearest neighbor Si−H sites (circles) (Figure 10). Such a geometry could be achieved through steric inhibition of nearest neighbor Si−H groups by the thermal rotation of the $-CH_3$ group about the Si−O bond. A long-range periodicity, such as that depicted in Figure 10, most likely cannot be achieved on real surfaces due to the putative random surface reaction,[90] but local $Si-OCH_3$ sites on a real surface may be surrounded by approximately 6 Si−H groups.

The experimentally observed limiting coverage of ∼30% for the $Si-OCH_3$ sites is interesting on another front because it contrasts with theoretical modeling, which predicts that the lowest surface strain is obtained for 100% coverage of methoxyl species.[91] The low strain at 100% coverage is due to the Coulombic attraction between neighboring $Si-OCH_3$ groups. This modeling did not, however, take into consideration the steric or energetic limitations of the transition state for the reaction of methanol on H−Si(111). Thus, while 100% coverage of the surface by $Si-OCH_3$ sites may exhibit less total strain than the 30% coverage observed in this work, it appears to be inaccessible, at least via a 65 °C reaction with neat anhydrous methanol, possibly due to steric restrictions of the transition state.

B. Mechanistic Remarks. ***1. Hydrogen-Terminated Si(111) Surfaces.*** Because virtually oxide-free methoxylated surfaces up to ∼30% of a monolayer can be prepared, the formation of subsurface Si−O−Si modes is not inherent to the reaction with methanol. Specifically, one could envision reaction products being $Si_2(Si-O)Si-CH_3$ and H_2 (g), where the oxygen atom from the methanol molecule ends up in one of the three Si−Si back bonds, leaving an atop $Si-CH_3$ group. In addition to the absence of Si−O−Si modes on the 65 °C reaction with H−Si(111) surfaces, no evidence for $Si-CH_3$ modes has been observed. $Si-CH_3$ surfaces has been studied in great detail using FTIR,[11,109,100] and no peaks in the region of $Si-CH_3$ umbrella distortion (757 cm^{-1}) or the $Si-CH_3$ rocking mode (1257 cm^{-1}) have been observed out of the noise in this study. Such a surface reaction on Si(111) surfaces thus cannot occur with a significant contribution to the total surface coverage under these conditions.

2. Hydroxy-Terminated Oxide Surfaces. Several reaction mechanisms can be proposed on the basis of the FTIR data

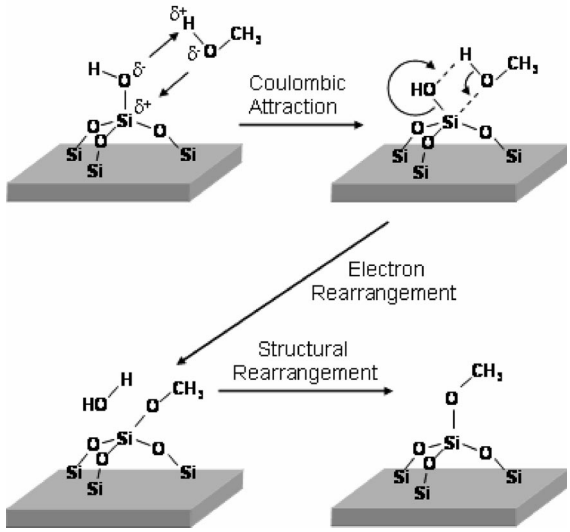

Figure 11. Possible reaction mechanism for the methoxylation of hydroxy-terminated oxide surface sites.

presented in this work. Figure 11 presents a possible reaction mechanism for the methoxylation of hydroxy-terminated surface sites on a SiO_2 oxide layer. Hydrogen bonding and Coulombic attraction bring the methanol molecule close to the surface hydroxyl (Si−OH) site such that it forms a four-membered-ring transition state as depicted. This transition state involves a pentavalent coordinate geometry for silicon. Although penta- and hexa-coordinated silicon atoms occur for free molecules in solution,[92] such geometries have only been assumed for silicon atoms bound in a surface lattice.[51,62,93] This transition state, however, is the lowest in energy of DFT calculations[94] and is supported by FTIR measurements of isotopically labeled CH_3OH molecules exposed to a SiO_2 surface.[95] From the putative transition state (Figure 11), electronic and structural rearrangements result in the formation of the methoxylated surface and the release of a water molecule. Despite the hydrophilic nature of the oxide surface, preferential adsorption of CH_3OH over H_2O has been observed for surface energy reasons. Thus, despite the release of H_2O during the methoxylation reaction, continued reaction with methanol is expected.[95]

3. Hydrogen-Terminated Oxide Surfaces. The formation of hydrogen- or alkyl-terminated oxide surfaces has been the focus of many studies. Of critical importance to the resulting film structure[96,97] is the amount of water on the oxide surface prior to treatment. This water layer is usually at least several monolayers thick;[43] suface-bound water cannot be fully removed without a high-temperature treatment,[98] which can result in the dehydration of the oxide into strained siloxane bridges.[95] The siloxane film is considered to be quite disordered with some Si−O−Si bonds linking neighboring molecules together and other Si−O−Si bonds linking some molecules to the surface.

Analogously, the FTIR spectrum of the TCS-treated oxide surface (Figure 6b) demonstrates the increase in at least two types of Si−O−Si bonds: some that are coupled in vibration to the Si−O−Si TO and LO modes of the surface oxide (1050 and 1260 cm^{-1}), and some that are not coupled to these modes (∼1090 and ∼1160 cm^{-1}). Due to the close physical proximity required for mode coupling, as well as the nonreactivity of these modes with methanol (vida infra), we propose that the LO- and TO-coupled Si−O−Si modes result from TCS molecules that add Si−O−Si bonds that physically complete the bulk of the SiO_2 matrix. Condensation reactions between hydrolyzed TCS molecules will likely form a Si−O−Si network that will not

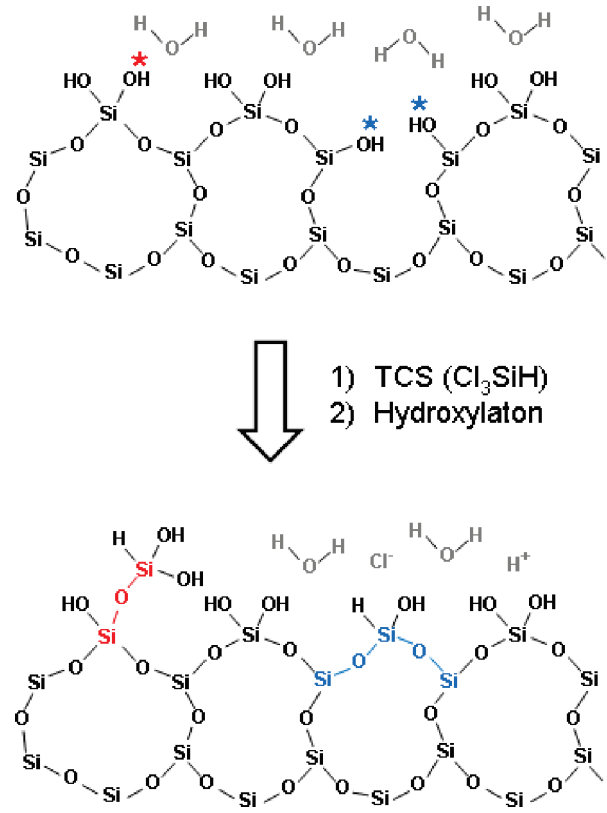

Figure 12. Schematic for the reaction of TCS with an oxide surface. TCS molecules reacting at the sites labeled by blue stars would complete an extended network of the Si−O−Si bulk, presumably increasing the absorption of the SiO_2 LO and TO modes. TCS molecules reacting at the red star may not lead to an increase in the LO and TO modes. Due to steric reasons, the blue Si−O−Si bonds would be less accessible for attack by CH_3OH relative to the red Si−O−Si moiety. For clarity, this model is two-dimensional.[99]

couple to the bulk modes of the oxide surface. This concept is depicted graphically in Figure 12 in a two-dimensional format.[99] When a molecule of TCS reacts at the positions indicated by the two blue stars, the two resulting Si−O−Si bonds complete an extended network of the bulk SiO_2 matrix, increasing the absorption of the TO and LO Si−O−Si modes. If a free TCS molecule, or a cluster of condensed molecules, reacts at the single red star, an isolated Si−O−Si bond likely forms.

This assignment is based on the following reasons. First, sol−gel synthesis of silica from $Si(OR)_4$ siloxanes is believed to produce ring structures with either 4 or 6 Si−O repeat units with a roughly 80−90% preference for the 4-ring species.[100,101] The 4-ring structures have been reported to produce FTIR LO and TO modes at ∼1160 and ∼1080 cm^{-1}, respectively; these values are very similar to the uncoupled Si−O−Si modes observed in this work, implying that the TCS film is made of predominantly 4-ring structures. The 6-ring structures produce LO and TO modes at 1220 and 1040 cm^{-1}, respectively. The mode observed at ∼1260 cm^{-1} (Figure 6b) is, thus, too high in energy to be explained by the presence of 6-ring structures. Second, the difference in reactivity of these modes is also consistent with the model of Figure 12. Baum and Schiffrin have proposed that the number of bonds to a crystal lattice restricts the ability of that silicon atom to engage in hypervalent transition states.[102] The coupled Si−O−Si bonds, which are assumed to form a more intergral part of the physical SiO_2 matrix, are expected to be less reactive toward methanol based on the difficulty of that Si atom to reach a pentavalent transistion state necessary for reaction (Figure 11). In contrast, the

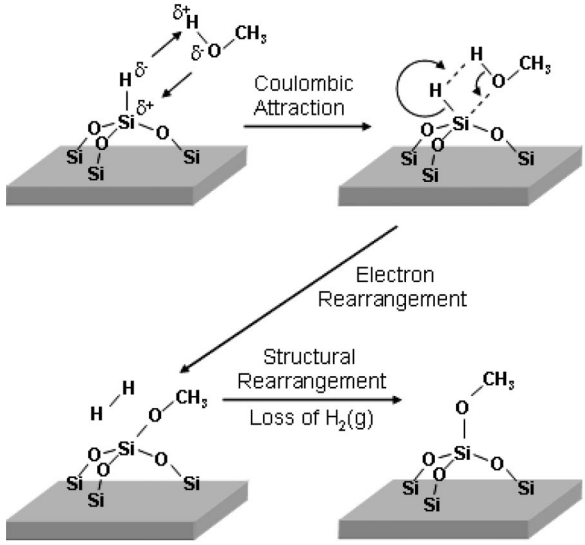

Figure 13. Possible mechanism for the reaction of a hydrogen-terminated oxide surface site with methanol.

uncoupled Si−O−Si bonds have a much higher reactivity with methanol. This hypothesis is also consistent with DFT calculations.[94] The energy needed to reach the transistion state for the reaction of a surface Si−OH site of an oxide layer with methanol is within 5% of that needed for a free Si−O−Si group (not constrained by the geometry of an oxide lattice). Thus, it appears that it is the tight crystal structure of the SiO_2 oxide matrix that prohibits the reaction of CH_3OH (l) with the LO- and TO-coupled Si−O−Si bonds.

If the oscillator strengths of the coupled and uncoupled Si−O−Si species are similar, a simple area comparison suggests that the overlayer created by the TCS is not very densely packed and/or not very physically connected with the bulk of the surface oxide layer. (See the Supporting Information section for more information.) The bonding geometry of trichlorosilane molecules to oxide surfaces has been subject to significant debate. Some reports claim that no direct bonds to the oxide surface are formed, but rather a plane of polymerized siloxanes forms that is separated from the surface by a few monolayers of water.[81,96] Meanwhile, other reports imply that a direct surface reaction has indeed occurred through X-ray photoelectron spectroscopy and secondary ion mass spectroscopy.[41] We believe that the increase in bulk Si−O−Si TO (1050 cm^{-1}) and LO (1260 cm^{-1}) modes provides strong evidence for the formation of at least some direct bonding to the surface.

Upon the reaction of the hydrogen-terminated oxide surface with methanol, a significant portion of the O_xSi-H stretching, the O_xSi-H bending modes, and the isolated Si−O−Si modes disappear. These observations can be explained by two possible reaction mechanisms (Figures 13 and 14). In Figure 13, the atop Si−H bond reacts exactly as has been proposed previously for Si−H sites on an atomically smooth hydrogen-terminated Si(111) sample.[59] Although this mechanism may be partly responsible for the observed loss in the Si−H modes upon the reaction with methanol, it cannot explain the significant loss in the uncoupled Si−O−Si modes.

The mechanism in Figure 14 describes a possible reaction of methanol with the uncoupled Si−O−Si back bonds such that the H-containing Si atom is removed (or etched) from the surface.[103] The chemistry of the resulting surface site will be different, however, depending on which Si atom of the Si−O−Si back-bond is attacked by the methanol. The reaction pathway

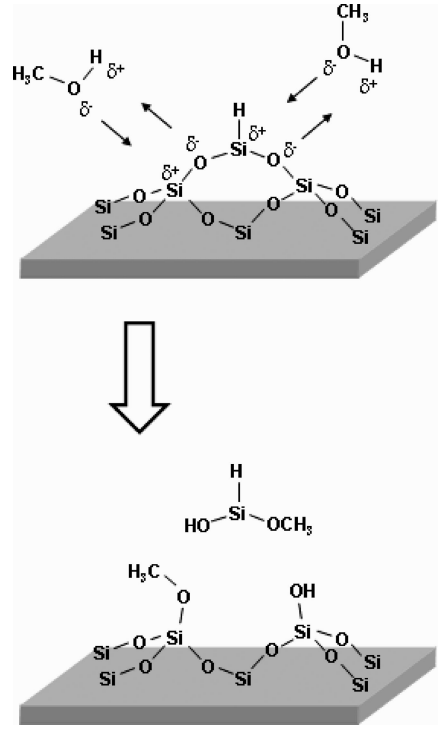

Figure 14. Possible mechanisms for the reaction of methanol with the hydrogen-terminated oxide surface in which the uncoupled/isolated Si−O−Si bonds are attacked. Depending on where the methanol attacks, the resulting surface site is either methoxy- or hydroxy-terminated. Since the silicon atom bound to H is removed from the surface in either case, a decrease in the Si−H intensity is expected even if the Si−H bond is not directly attacked. For clarity, the fourth bond of the atop silicon atom is omitted.

on the left depicts the electron pair of the oxygen atom in the methanol attacking the lower silicon atom, and the surface will be left with an atop $Si-OCH_3$ group. The remaining surface site is left hydroxyl terminated if the methanol attacks the atop silicon atom of the Si−O−Si linkage, as depicted by the pathway on the right. The remaining Si−OH site could, however, react further with CH_3OH (l) according to Figure 11. Thus, the hydrogen-terminated or hydroxy-terminated oxide surfaces result in similar FTIR signatures after reaction with methanol (Figure 7). Since the upper H-containing silicon atom is removed from the surface in either case, a decrease in the Si−H intensity is expected even if the Si−H bond is not directly attacked. Thus, we have no independent evidence that the mechanism presented in Figure 13 actually occurs under these conditions. For the purposes of investigating the reactivity of O_xSi-H sites with CH_3OH (l), we suggest that future experiments be performed on O_xSi-H surfaces formed from the reaction of H−Si(111) with O_2(g) at elevated temperatures.[76] Such surfaces are not expected to exhibit subsurface Si−O−Si reactivity with methanol, and reaction rates for atop O_xSi-H groups should be relatively uncomplicated.

The high reactivity of the isolated Si−O−Si species means that siloxane films made from similar trichlorosilane molecules will not lead to stable SAMs. If the Si−O−Si linkages must complete part of the bulk matrix of SiO_2 in order to be stable, only a few linkers will remain after immersing the sample into an alcohol or any other OH-containing liquid (such as H_2O).

4. Mechanisms for Subsurface Oxidation. The results presented thus far are consistent with the presence of Si−O−Si oxidation underneath atop $Si-OCH_3$ sites and not underneath Si−H sites. This unusually high selectivity in the position of

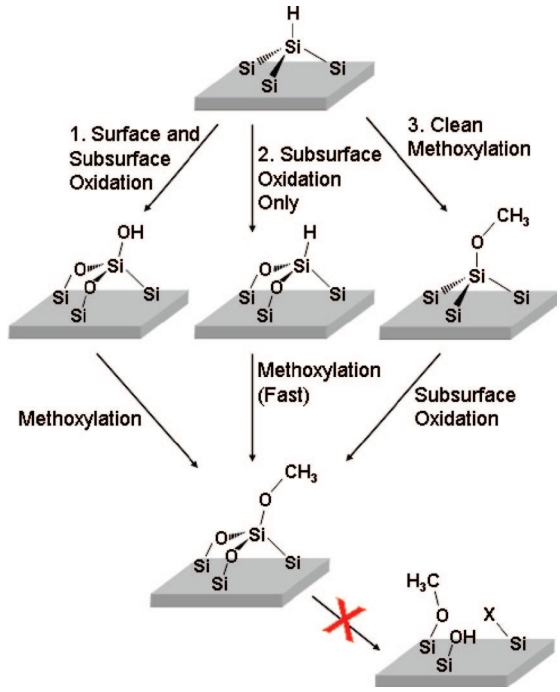

Figure 15. Possible mechanisms for the high selectivity of oxygen underneath regions of methoxyl groups. It seems extremely unlikely that methanol could further react with subsurface Si−O−Si bonds, as per Figure 14, because the resulting three functional groups, on the three subsurface silicon atoms, would have to fit into the space previously occupied by the single silicon atom.

the subsurface oxidation suggests that it has a chemical rather than a stochastic origin. The possible mechanisms for forming such a position-specific oxidation during the methanol reaction are outlined in Figure 15. Pathway 1 depicts the possibility that oxide-free H−Si(111) samples could be oxidized first (by any impurities such as O_2 or H_2O), such that both the subsurface Si−Si bonds and the atop Si−H bond are oxidized to Si−O−Si and Si-OH species, respectively. This hydroxy-terminated surface site can then be methoxylated as described in Figure 11. Increases in the SiO−H stretching mode (around 3700 cm^{-1}) have not been reliably observed, but difficulties in the water vapor subtraction within this region do not allow for a conclusive argument from our data to be made. Similarly, the bending mode for SiO−H groups, around 800−1000 cm^{-1}, has also never been observed for any of the (nonoxide-terminated) samples studied in this work, but this mode is expected to be fairly weak and broad. Thus, a significant surface concentration of the O_xSi−OH intermediate may fall below the detection limit. Pathway 2 depicts the possible mechanism in which only the subsurface Si−Si back bonds are oxidized to form a O_xSi−H site. This atop Si−H bond can then react with methanol as described in Figure 13. If this mechanism does occur, the reactivity of the O_xSi−H site to methanol must be significantly fast since no O_xSi−H bonds are observed experimentally; in this case, the sensitivity for the detection of O_xSi−H bonds is fairly high since the stretching mode is relatively intense (Figure 6b). Pathway 3 depicts the possibility that an oxide-free Si−OCH_3 surface site is created first, but the presence of the electronegative O atom weakens the Si−Si back bonds such that oxidation is facilitated after methoxylation.[104–108] Based on the steric and lattice arguments of Baum and Schiffrin, it seems extremely unlikely that methanol could further react with the subsurface Si−O−Si back bonds, which are already more strained the individual Si−Si back bonds. This hypothesis is in agreement with the result that a partially oxidized methoxyl surface exposed to 65 °C methanol for 10 h did not remove any Si−O−Si (Figure 8b).

V. Conclusions

Atomically smooth hydrogen-terminated Si(111) surfaces present a homogeneous bonding environment that, when coupled with high resolution FTIR measurements and a small reactant such as methanol, allow an investigation of the subtle shifts in vibrational modes that can unlock several key aspects regarding the chemistry of silicon surfaces. Specifically, homogeneous Si(111) surfaces with ∼30% Si−OCH_3 and ∼70% Si−H sites have been generated with no detectable subsurface oxidation (less than 3% of a monolayer) using a 65 °C reaction in neat CH_3OH (l). Such surfaces display vibrational modes that are sufficiently sharp to allow quantitative comparison with similarly reacted SiO_2 surfaces. Subsurface oxidation has been observed for room temperature reactions with neat alcohol, or upon deliberate exposure of methoxylated surfaces to laboratory air followed by a subsequent exposure to neat CH_3OH. The FTIR spectra of these oxide-containing samples all display blue-shifted components of the complex O−C, umbrella CH_3, and C−H stretching modes. These modes are assigned to O_xSi−OCH_3 sites and are corroborated by DFT calculations. While it is unclear what fraction of surface oxide may by hydroxy-terminated (based on a low sensitivity for this surface species), we have demonstrated experimentally that oxide, when present, is at least partially terminated by Si−OCH_3 sites and not Si−H sites. In contrast to H−Si(111) surfaces, H−Si(100) surfaces under the same reaction conditions exhibit significant surface oxidization. The lower reactivity, more-controllable, and atomically smooth Si(111) surface thus demonstrates superior properties that can be harnessed for nanoelectronic applications. Finally, hydrogen-terminated oxide surfaces formed with trichlorosilane are quite unstable upon exposure to methanol.

Acknowledgment. We acknowledge the support of the National Science Foundation, through Grant CHE-0415652 at Rutgers and UT Dallas, and through the U.S.−France cooperative research program (NSF-INT-0341053) for facilitating the international collaboration with the LAAS at Toulouse, and associated CALMIP computer resources. The authors are grateful to Nathan S. Lewis for stimulating discussions.

Supporting Information Available: Additional experimental details and analysis. This material is available free of charge via the Internet at http://pubs.acs.org.

References and Notes

(1) Eades, W. D.; Swanson, R. M. *J. Appl. Phys.* **1985**, *58*, 4267.
(2) Nicollian, E. H.; Goetzberger, A. *Bell Syst. Tech. J.* **1967**, *46*, 1055.
(3) Royea, W. J.; Michalak, D. J.; Lewis, N. S. *Appl. Phys. Lett.* **2000**, *77*, 2566.
(4) Janshoff, A.; Dancil, K. P. S.; Steinem, C.; Greiner, D. P.; Lin, V. S. Y.; Gurtner, C.; Motesharei, K.; Sailor, M. J.; Ghadiri, M. R. *J. Am. Chem. Soc.* **1998**, *120*, 12108.
(5) Canham, L. T.; Stewart, M. P.; Buriak, J. M.; Reeves, C. L.; Anderson, M.; Squire, E. K.; Allcock, P.; Snow, P. A. *Phys. Status Solidi A-Appl. Res.* **2000**, *182*, 521.
(6) Haick, H.; Hurley, P. T.; Hochbaum, A. I.; Yang, P. D.; Lewis, N. S. *J. Am. Chem. Soc.* **2006**, *128*, 8990.
(7) Buriak, J. M. *Chem. Rev.* **2002**, *102*, 1271.
(8) Filler, M. A.; Bent, S. F. *Prog. Surf. Sci.* **2003**, *73*, 1.
(9) Webb, L. J.; Lewis, N. S. *J. Phys. Chem. B* **2003**, *107*, 5404.
(10) Webb, L. J.; Nemanick, E. J.; Biteen, J. S.; Knapp, D. W.; Michalak, D. J.; Traub, M. C.; Chan, A. S. Y.; Brunschwig, B. S.; Lewis, N. S. *J. Phys. Chem. B* **2005**, *109*, 3930.

(11) Webb, L. J.; Rivillon, S.; Michalak, D. J.; Chabal, Y. J.; Lewis, N. S. *J. Phys. Chem. B* **2006**, *110*, 7349.

(12) Sieval, A. B.; Huisman, C. L.; Schonecker, A.; Schuurmans, F. M.; van der Heide, A. S. H.; Goossens, A.; Sinke, W. C.; Zuilhof, H.; Sudholter, E. J. R. *J. Phys. Chem. B* **2003**, *107*, 6846.

(13) Nemanick, E. J.; Hurley, P. T.; Brunschwig, B. S.; Lewis, N. S. *J. Phys. Chem. B* **2006**, *110*, 14800.

(14) Nemanick, E. J.; Hurley, P. T.; Webb, L. J.; Knapp, D. W.; Michalak, D. J.; Brunschwig, B. S.; Lewis, N. S. *J. Phys. Chem. B* **2006**, *110*, 14770.

(15) Webb, L. J.; Michalak, D. J.; Biteen, J. S.; Brunschwig, B. S.; Chan, A. S. Y.; Knapp, D. W.; Meyer, H. M.; Nemanick, E. J.; Traub, M. C.; Lewis, N. S. *J. Phys. Chem. B* **2006**, *110*, 23450.

(16) Dancil, K. P. S.; Greiner, D. P.; Sailor, M. J. *J. Am. Chem. Soc.* **1999**, *121*, 7925.

(17) Maldonado, S.; Plass, K. E.; Knapp, D.; Lewis, N. S. *J. Phys. Chem. C* **2007**, *111*, 17690.

(18) Smalley, J. F.; Sachs, S. B.; Chidsey, C. E. D.; Dudek, S. P.; Sikes, H. D.; Creager, S. E.; Yu, C. J.; Feldberg, S. W.; Newton, M. D. *J. Am. Chem. Soc.* **2004**, *126*, 14620.

(19) Cheng, J.; Robinson, D. B.; Cicero, R. L.; Eberspacher, T.; Barrelet, C. J.; Chidsey, C. E. D. *J. Phys. Chem. B* **2001**, *105*, 10900.

(20) Barrelet, C. J.; Robinson, D. B.; Cheng, J.; Hunt, T. P.; Quate, C. F.; Chidsey, C. E. D. *Langmuir* **2001**, *17*, 3460.

(21) Sailor, M. J.; Lee, E. J. *Adv. Mater.* **1997**, *9*, 783.

(22) Pomykal, K. E.; Fajardo, A. M.; Lewis, N. S. *J. Phys. Chem.* **1995**, *99*, 8302.

(23) Parker, E. E.; Ashurst, W. R.; Carraro, C.; Maboudian, R. *J. Microelectromech. Syst.* **2005**, *14*, 947.

(24) Maboudian, R.; Carraro, C. *Annu. Rev. Phys. Chem.* **2004**, *55*, 35.

(25) Ashurst, W. R.; Carraro, C.; Maboudian, R.; Frey, W. *Sens. Actuators A-Phys.* **2003**, *104*, 213.

(26) Ciampi, S.; Bocking, T.; Kilian, K. A.; James, M.; Harper, J. B.; Gooding, J. J. *Langmuir* **2007**, *23*, 9320.

(27) Waggoner, P. S.; Craighead, H. G. *Lab Chip* **2007**, *7*, 1238.

(28) Yin, H. B.; Brown, T.; Greef, R.; Wilkinson, J. S.; Melvin, T. *Microelectron. Eng.* **2004**, *73*−*74*, 830.

(29) Boukherroub, R.; Wayner, D. D. M. *J. Am. Chem. Soc.* **1999**, *121*, 11513.

(30) Asanuma, H.; Lopinski, G. P.; Yu, H. Z. *Langmuir* **2005**, *21*, 5013.

(31) Voicu, R.; Boukherroub, R.; Bartzoka, V.; Ward, T.; Wojtyk, J. T. C.; Wayner, D. D. M. *Langmuir* **2004**, *20*, 11713.

(32) Frechette, J.; Maboudian, R.; Carraro, C. *J. Microelectromech. Syst.* **2006**, *15*, 737.

(33) Frechette, J.; Maboudian, R.; Carraro, C. *Langmuir* **2006**, *22*, 2726.

(34) Etienne, M.; Walcarius, A. *Talanta* **2003**, *59*, 1173.

(35) Wang, J.; Guo, D. J.; Xia, B.; Chao, J.; Xiao, S. J. *Colloids Surf. A* **2007**, *305*, 66.

(36) Eves, B. J.; Fan, C. Y.; Lopinski, G. P. *Small* **2006**, *2*, 1379.

(37) Brewer, R. T.; Ho, M. T.; Zhang, K. Z.; Goncharova, L. V.; Starodub, D. G.; Gustafsson, T.; Chabal, Y. J.; Moumen, N. *Appl. Phys. Lett.* **2004**, *85*, 3830.

(38) Nemanick, E. J.; Solares, S. D.; Goddard, W. A.; Lewis, N. S. *J. Phys. Chem. B* **2006**, *110*, 14842.

(39) Wen, Y. Q.; Yi, W. H.; Meng, L. J.; Feng, M.; Jiang, G. Y.; Yuan, W. F.; Zhang, Y. Q.; Gao, H. J.; Jiang, L.; Song, Y. L. *J. Phys. Chem. B* **2005**, *109*, 14465.

(40) Elmore, D. L.; Chase, D. B.; Liu, Y. J.; Rabolt, J. F. *Vib. Spectrosc.* **2004**, *34*, 37.

(41) Rye, R. R.; Nelson, G. C.; Dugger, M. T. *Langmuir* **1997**, *13*, 2965.

(42) Jal, P. K.; Patel, S.; Mishra, B. *Talanta* **2004**, *62*, 1005.

(43) Allara, D. L.; Parikh, A. N.; Rondelez, F. *Langmuir* **1995**, *11*, 2357.

(44) Jeon, N. L.; Choi, I. S.; Whitesides, G. M.; Kim, N. Y.; Laibinis, P. E.; Harada, Y.; Finnie, K. R.; Girolami, G. S.; Nuzzo, R. G. *Appl. Phys. Lett.* **1999**, *75*, 4201.

(45) Boukherroub, R.; Morin, S.; Sharpe, P.; Wayner, D. D. M.; Allongue, P. *Langmuir* **2000**, *16*, 7429.

(46) Chazalviel, J. N. *J. Electroanal. Chem.* **1987**, *233*, 37.

(47) Warntjes, M.; Vieillard, C.; Ozanam, F.; Chazalviel, J. N. *J. Electrochem. Soc.* **1995**, *142*, 4138.

(48) Cleland, G.; Horrocks, B. R.; Houlton, A. *J. Chem. Soc.-Faraday Trans.* **1995**, *91*, 4001.

(49) Bateman, J. E.; Eagling, R. D.; Horrocks, B. R.; Houlton, A. *J. Phys. Chem. B* **2000**, *104*, 5557.

(50) Bateman, J. E.; Horrocks, B. R.; Houlton, A. *J. Chem. Soc.-Faraday Trans.* **1997**, *93*, 2427.

(51) Haber, J. A.; Lauermann, I.; Michalak, D.; Vaid, T. P.; Lewis, N. S. *J. Phys. Chem. B* **2000**, *104*, 9947.

(52) Hacker, C. A.; Anderson, K. A.; Richter, L. J.; Richter, C. A. *Langmuir* **2005**, *21*, 882.

(53) Zhu, X. Y.; Boiadjiev, V.; Mulder, J. A.; Hsung, R. P.; Major, R. C. *Langmuir* **2000**, *16*, 6766.

(54) Higashi, G. S.; Becker, R. S.; Chabal, Y. J.; Becker, A. J. *Appl. Phys. Lett.* **1991**, *58*, 1656.

(55) Langner, A.; Panarello, A.; Rivillon, S.; Vassylyev, O.; Khinast, J. G.; Chabal, Y. J. *J. Am. Chem. Soc.* **2005**, *127*, 12798.

(56) Newton, T. A.; Huang, Y. C.; Lepak, L. A.; Hines, M. A. *J. Chem. Phys.* **1999**, *111*, 9125.

(57) Bomchil, G.; Herino, R.; Barla, K.; Pfister, J. C. *J. Electrochem. Soc.* **1983**, *130*, 1611.

(58) Kang, C. G.; Kang, M. S.; Yang, J. H.; Jin, J. H.; Hong, S. I.; Min, N. K. *J. Korean Phys. Soc.* **2003**, *42*, S693.

(59) Michalak, D. J.; Rivillon, S.; Chabal, Y. J.; Esteve, A.; Lewis, N. S. *J. Phys. Chem. B* **2006**, *110*, 20426.

(60) This detection limit was calculated using the average noise root-mean-square amplitude of 0.018 mAU over the spectral region of 920−1060 cm^{-1} for the oxide-free Si-OCH_3 samples and the 1.5 mAU intensity of the Si−O−Si TO mode (∼1050 cm^{-1}) observed on an SC1/SC2-cleaned surface that has a ∼6-Å (∼2 monolayer) thick oxide based on the Si−O−Si LO frequency of 1220 cm^{-1} (ref 71). An accurate calculation of the detection limit is difficult because the spectral features of the Si−O−Si TO mode may not remain linear with surface coverage at submonolayer concentrations.

(61) Higashi, G. S.; Chabal, Y. J.; Trucks, G. W.; Raghavachari, K. *Appl. Phys. Lett.* **1990**, *56*, 656.

(62) Hines, M. A. *Annu. Rev. Phys. Chem.* **2003**, *54*, 29.

(63) Frisch, M. J.; Trucks, G. W.; Schlegel, H. B.; Scuseria, G. E.; Robb, M. A.; Cheeseman, J. R.; Montgomery, J. A.; Vreven, T.N., K. K.; Burant, J. C.; Millam, J. M.; Iyengar, S. S.; Tomasi, J.; Barone, V.; Mennucci, B.; Cossi, M.; Scalmani, G.; Rega, N.; Petersson, G. A.; Nakatsuji, H.; Hada, M.; Ehara, M.; Toyota, K.; Fukuda, R.; Hasegawa, J.; Ishida, M.; Nakajima, T.; Honda, Y.; Kitao, O.; Nakai, H.; Klene, M.; Li, X.; Knox, J. E.; Hratchian, H. P.; Cross, J. B.; Adamo, C.; Jaramillo, J.; Gomperts, R.; Stratmann, R. E.; Yazyev, O.; Austin, A. J.; Cammi, R.; Pomelli, C.; Ochterski, J. W.; Ayala, P. Y; Morokuma, K.; Voth, G. A.; Salvador, P.; Dannenberg, J. J.; Zakrzewski, V. G.; Dapprich, S.; Daniels, A. D.; Strain, M. C.; Farkas, O.; Malick, D. K.; Rabuck, A. D.; Raghavachari, K.; Foresman, J. B.; Ortiz, J. V.; Cui, Q.; Baboul, A. G.; Clifford, S.; Cioslowski, J; Stefanov, B. B.; Liu, G.; Liashenko, A.; Piskorz, P.; Komaromi, I.; Martin, R. L; Fox, D. J.; Keith, T.; Al-Laham, M. A.; Peng, C. Y.; Nanayakkara, A.; Challacombe, M.; Gill, P. M. W.; Johnson, B.; Chen, W.; Wong, M. W.; Gonzalez, C.; Pople, J. A. *Gaussian 03*, revision B.05; Gaussian, Inc.: Pittsburgh, PA, 2003.

(64) Becke, A. D. *J. Chem. Phys.* **1993**, *98*, 5648.

(65) Lee, C. T.; Yang, W. T.; Parr, R. G. *Phys. Rev. B* **1988**, *37*, 785.

(66) Pelmenschikov, A. G.; Morosi, G.; Gamba, A.; Zecchina, A.; Bordiga, S.; Paukshtis, E. A. *J. Phys. Chem.* **1993**, *97*, 11979.

(67) Jakob, P.; Chabal, Y. J.; Raghavachari, K. *Chem. Phys. Lett.* **1991**, *187*, 325.

(68) Jakob, P.; Chabal, Y. J.; Raghavachari, K.; Christman, S. B. *Phys. Rev. B* **1993**, *47*, 6839.

(69) Jakob, P.; Chabal, Y. J.; Raghavachari, K.; Dumas, P.; Christman, S. B. *Surf. Sci.* **1993**, *285*, 251.

(70) Luo, H. H.; Chidsey, C. E. D. *Appl. Phys. Lett.* **1998**, *72*, 477.

(71) Queeney, K. T.; Chabal, Y. J.; Weldon, M. K.; Raghavachari, K. *Phys. Status Solidi A-Appl. Res.* **1999**, *175*, 77.

(72) Queeney, K. T.; Herbots, N.; Shaw, J. M.; Atluri, V.; Chabal, Y. J. *Appl. Phys. Lett.* **2004**, *84*, 493.

(73) Queeney, K. T.; Weldon, M. K.; Chang, J. P.; Chabal, Y. J.; Gurevich, A. B.; Sapjeta, J.; Opila, R. L. *J. Appl. Phys.* **2000**, *87*, 1322.

(74) Weldon, M. K.; Queeney, K. T.; Chabal, Y. J.; Stefanov, B. B.; Raghavachari, K. *J. Vac. Sci. Technol. B* **1999**, *17*, 1795.

(75) Neuwald, U.; Hessel, H. E.; Feltz, A.; Memmert, U.; Behm, R. J. *Appl. Phys. Lett.* **1992**, *60*, 1307.

(76) Zhang, X.; Chabal, Y. J.; Christman, S. B.; Chaban, E. E.; Garfunkel, E. *J. Vac. Sci. Technol. A* **2001**, *19*, 1725.

(77) At this point, we are unable to determine if the consistent absence of Si−O−Si modes observed at 65 °C is due to inherent chemical or kinetic reasons, lower gas solubility at elevated temperatures, or enhanced cleanliness of the glassware due to the rinsing treatment with hot methanol. Nevertheless, the spectra demonstrate that it is possible to generate a methoxylated surface without any detectable oxide.

(78) The Si(100) surface is considerably more rough than the Si(111) surface, so the increase in intensity of these modes may not necessarily correspond to a higher coverage per available surface sites. In addition, the orientation of the resulting Si−OCH_3 species with repect to the surface normal may also be different for the two surfaces, and this could lead to changes in the infrared absorption for a given light incidence angle even for the same surface coverage. Finally, the higher reactivity of the Si(100) surface could presumably lead to a higher coverage of Si−OCH_3 sites. For these reasons, a direct comparison of the surface coverage of Si−OCH_3 sites for the Si(111) and Si(100) surfaces based on the data presented herein is not trivial.

(79) Chabal, Y. J.; Higashi, G. S.; Raghavachari, K.; Burrows, V. A. *J. Vac. Sci. Technol. A* **1989**, *7*, 2104.

(80) Dumas, P.; Chabal, Y. J.; Jakob, P. *Surf. Sci.* **1992**, *270*, 867.

(81) Tripp, C. P.; Hair, M. L. *Langmuir* **1995**, *11*, 149.

(82) This decrease in Si−OH mode is surprising because hydrolyzed TCS molecules have 3 Si−OH groups per molecule. Thus, a decrease in the Si−OH mode intensity either implies that the unreacted Si−OH modes are highly screened out by the oxide film or that the siloxane film is highly crosslinked (more than two Si−OH sites per TCS molecule are condensed to form the Si−O−Si network).

(83) Upon closer inspection, spectra a and c in Figure 8 do contain small components of blue shifted modes which may indicate that the surface is not entirely oxide free; an analysis of the amount of blue-shifted modes may thus provide a lower detection limit on amount of subsurface oxidation than the presence of Si−O−Si LO and TO modes.

(84) Rivillon, S.; Brewer, R. T.; Chabal, Y. J. *Appl. Phys. Lett.* **2005**, 87.

(85) Rao, G. R.; Wang, Z. H.; Watanabe, H.; Aoyagi, M.; Urisu, T. *Surf. Sci.* **2004**, *570*, 178.

(86) Zhang, X.; Garfunkel, E.; Chabal, Y. J.; Christman, S. B.; Chaban, E. E. *Appl. Phys. Lett.* **2001**, *79*, 4051.

(87) Queeney, K. T.; Weldon, M. K.; Chabal, Y. J.; Raghavachari, K. *J. Chem. Phys.* **2003**, *119*, 2307.

(88) Gstrein, F.; Michalak, D. J.; Royea, W. J.; Lewis, N. S. *J. Phys. Chem. B* **2002**, *106*, 2950.

(89) Rosenbluth, M. L.; Lewis, N. S. *J. Am. Chem. Soc.* **1986**, *108*, 4689.

(90) A long-range periodicity as described in Figure 9 would require one of two possibilities. First, for a terrace-top reaction mechanism, the reactivity of a lone Si−H site must be much less than the reactivity of a second-nearest-neighbor Si−H site to a $Si-OCH_3$ group (i.e., such that the nucleation rate is slow relative to the growth of a domain edge). Possibilities for such selectivity include an increased polarization of the second-nearest-neighbor Si−H group due to the presence of the Si−O bond of the $Si-OCH_3$ group, or the increased residence time of the solution-phase methanol molecule at the second-nearest-neighbor site based on van der Waals attraction between two CH_3 groups. The polarization of the second nearest neighbor Si−H group is expected to be small; periodic boundary array calculations by Solares et al. (ref 91) show that the atomic charge on a silicon atom four lattice sites into the crystal (which corresponds to the same distance as a second nearest neighbor atop site) is negligible. Both the CH_3 terminus of the $Si-OCH_3$ group and the Si−H sites of the surface are non-polar so a significantly larger residence time of a CH_3OH molecule near the $Si-OCH_3$ site seems unlikely. Reactions on the terrace top, thus seem unlikey to lead to any long range periodicity. Second, a step-flow mechanism for the formation of methoxyl-terminated surfaces has been proposed by Michalak et al. (ref 59). Steric limitations along the step edge during the putative step-flow reaction, if it occurs, could however lead to a more periodic surface coverage.

(91) Solares, S. D.; Michalak, D. J.; Goddard, W. A.; Lewis, N. S. *J. Phys. Chem. B* **2006**, *110*, 8171.

(92) Chuit, C.; Corriu, R. J. P.; Reye, C.; Young, J. C. *Chem. Rev.* **1993**, *93*, 1371.

(93) Hines, M. A.; Chabal, Y. J.; Harris, T. D.; Harris, A. L. *J. Chem. Phys.* **1994**, *101*, 8055.

(94) Natal-Santiago, M. A.; Dumesic, J. A. *J. Catal.* **1998**, *175*, 252.

(95) Wovchko, E. A.; Camp, J. C.; Glass, J. A.; Yates, J. T. *Langmuir* **1995**, *11*, 2592.

(96) Tripp, C. P.; Hair, M. L. *Langmuir* **1992**, *8*, 1120.

(97) Parikh, A. N.; Allara, D. L.; Azouz, I. B.; Rondelez, F. *J. Phys. Chem.* **1994**, *98*, 7577.

(98) Zhuravlev, L. T. *Langmuir* **1987**, *3*, 316.

(99) An accurate representation of a three dimensional oxide surface would have an average of 4 oxygen atoms around each silicon atom and two silicon atoms around each oxygen atom.

(100) Fidalgo, A.; Ciriminna, R.; Ilharco, L. M.; Pagliaro, M. *Chem. Mater.* **2005**, *17*, 6686.

(101) Fidalgo, A.; Ilharco, L. M. *Chem.−Eur. J.* **2004**, *10*, 392.

(102) Baum, T.; Schiffrin, D. J. *J. Chem. Soc.-Faraday Trans.* **1998**, *94*, 691.

(103) For clarity, the fourth bond of the silicon atom in the atop Si−H site of Figure 13 was removed. In addition, Figure 13 is not intending to imply that silicon atop sites that contain two Si−O−Si linkages with the surface are reactive; such a geometry may already present a transition state that is too sterically inhibited to allow either of these mechanisms to occur.

(104) Zhang, R. Q.; Zhao, Y. L.; Teo, B. K. *Phys. Rev. B* **2004**, 69.

(105) Allongue, P.; Costa Kieling, V.; Gerischer, H. *J. Electrochem. Soc.* **1993**, *140*, 1009.

(106) Allongue, P.; Costa Kieling, V.; Gerischer, H. *J. Electrochem. Soc.* **1993**, *140*, 1018.

(107) Allongue, P.; Kieling, V.; Gerischer, H. *Electrochim. Acta* **1995**, *40*, 1353.

(108) Allongue, P.; Kieling, V.; Gerischer, H. *J. Phys. Chem.* **1995**, *99*, 9472.

(109) Amy, S. R.; Michalak, D. J.; Chabal, Y. J.; Wielunski, L.; Hurley, P. T.; Lewis, N. S. *J. Phys. Chem. C* **2007**, *111*, 13053.

JP8030539